Paper No. 02-2277

Experimental and Numerical Response of a 1915 Riveted Through-Girder Bridge

Daniel G. Linzell, Deanna L. Nevling, Adrian A. Kollias, and Jeffrey A. Laman

Chester County Bridge #21, a 16.5-m (54-ft), single-span, riveted, through-girder bridge located in upper Oxford Township, Pennsylvania, was field tested to determine the response to controlled loading. The bridge was instrumented with strain and displacement transducers to monitor response at critical locations as a single-axle truck of known weight was driven across the structure at crawl and posted speeds. Strains generated in the girders and in transverse floor beams supporting the deck were measured along with girder midspan vertical deflections. Information produced from the tests was used to (*a*) assess the level of composite action and load distribution in the structure and (*b*) determine if certain members are reaching critical stress levels and to determine the load rating. In addition, analytical models were developed both to predict the response and to evaluate the level of calibration required to establish a model that accurately reflected measured response.

Prediction of bridge live-load response is important for both improved design and accurate evaluation of existing bridge structures. Because of limited resources and aging bridge inventories, bridge owners are increasingly faced with decisions to post older bridges. It has been demonstrated that, for concrete-slab-on-steel-girder bridges, unforeseen composite action between the slab and girders often enhances their load-carrying capacity (*1–4*). This action is caused mainly by friction and chemical bond between the concrete deck and supporting superstructure, and it could be inferred that similar effects occur for many of the single-span, steel, through-girder bridges located on secondary and rural routes in the United States, although published research substantiating this assumption is currently limited. The present study examines the behavior of through-girder bridges by focusing on the structural evaluation of a 1915 bridge of common construction to accurately assess its live-load capacity.

Many existing bridge structures exhibit complex load paths that are difficult to predict with current modeling techniques. Bridge #21, which carries Muddy Run Road over Muddy Run in Chester County, Pennsylvania, was instrumented and tested on August 1, 2000, to measure levels of strain and deflections at critical locations on the steel through-girders and floor beams that support the concrete deck (*5*). The field tests monitored structural response as a truck of known weight was driven across the bridge at various locations and speeds. The collected strain and deflection data were reduced, examined, and used to

- Assess the level of composite action and load distribution in the structure,
- Determine the controlling members for rating of the bridge,
- Establish the current rating,
- Evaluate dynamic impact due to the test truck, and
- Make recommendations for future repairs to the concrete deck and steel girders and floor beams.

For the present study, a numerical analysis was performed for comparison with the measured response. The numerical model consisted of beam elements for the superstructure with plate elements to simulate the concrete deck. The model was evaluated under composite and noncomposite floor-beam and girder assumptions. Strain and deflection values at instrumented locations were generated from the model as a function of truck position. The purpose of the numerical model simulation was to

- Compare predictions from the numerical results with measured field results,
- Establish the accuracy with which numerical models can analyze and predict structural behavior under specified loading conditions,
- Compare predicted stresses under an assumption of composite action between the concrete deck and floor beams and girders in relation to the measured results, and
- Compare the influence of noncomposite and composite behavior on bridge strength and load capacity.

STRUCTURE DESCRIPTION

The bridge is a single-span, through-girder structure with an overall length of 16.5 m (54 ft) and a width of 6.1 m (20 ft) between girder webs. The girders span 15.8 m (51 ft 10¼ in.) between bearing supports, and the roadway width is 5.3 m (17 ft 6 in.). An elevation view (Figure 1) and schematic drawings of the bridge (Figures 2 and 3) are provided.

The through-girders are built-up steel sections consisting of four L 5 in. × 3½ in. × 11/16 in. riveted to 1.3- × 132.1-cm (½- × 52-in.) web plates. Cover plates measuring 1.3 × 30.5 cm (½ × 12 in.) are attached to the top and bottom flanges of the built-up section away from the supports, with the top flange having two cover plates placed over the interior 10.1 m (33 ft 3 in.) of the span and the bottom flange having one plate mounted over the interior 12.5 m (41 ft 0 in.) and a second over the interior 7.3 m (24 ft 0 in.) of the span. Transverse stiffeners are riveted to the girder web at each floor-beam connection point. Transverse floor beams are connected to each girder web near the girder bottom flange at a spacing of 1.2 m or 1.3 m (4 ft 1 or 2½ in.). The floor beams span 6.1 m (20 ft 0 in.) and are W12×45s. Attached to the center 3.7 m (12 ft) of each W12 floor-beam bottom flange is a 1.1- × 15.2-cm (7/16- × 6-in.) cover plate.

Directly above the beams is a cast-in-place concrete slab that varies between 16.5 cm (6½ in.) and 20.3 cm (8 in.) in thickness. The slab is overlaid with an 11.4-cm (4½-in.) bituminous wearing

Department of Civil and Environmental Engineering, The Pennsylvania State University, University Park, PA 16802-1408.

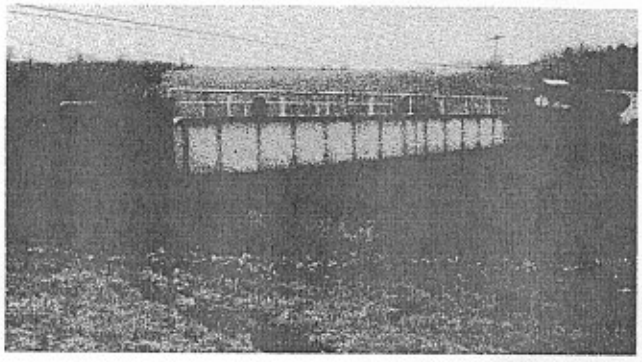

FIGURE 1 East elevation, Bridge #21.

surface. Concrete curbs with a height of 26.7 cm (10½ in.) and a width of 35.6 cm (14 in.) are poured along the edges of the slab. The structure was designed and built as a noncomposite system.

ASSESSMENT OF BRIDGE CONDITION

The condition assessment of the bridge is based on visual observations conducted before the field test, and assessment criteria were taken from federal bridge inventory and appraisal guidelines (*6*). The overall condition of the bridge is characterized as fair to poor. The concrete deck slab is in generally poor condition, with extensive rutting and cracking evident in the bituminous wearing surface, debris present along the curb line, and severe honeycombing and spalling with exposed and corroded reinforcing steel and extensive efflorescence evident on the underside. The floor beams are in generally fair to poor condition with many having extensive corrosion, pack rust, and loss of section near midspan because of deck leakage. The through-girders were observed to be in generally fair condition. The portion of each girder above the deck surface was in fair condition with general deterioration of the paint system being observed and isolated areas of corrosion near the curb line. The portion of each girder below the deck surface was more extensively deteriorated, with intermittent locations of corrosion observed on the webs and bottom flanges. No significant pack rust or loss of section was observed on either girder.

EXPERIMENTAL PROCEDURE

Strain and displacement measurement transducers were placed at critical locations of the through-girder and floor beams (see Figure 2) to measure strains and deformations under load. Bridge response to a single-axle truck traveling at crawl and posted speeds was monitored using a 16-bit, high-speed, data acquisition system. Strains were recorded using demountable strain transducers (STs) mounted to girders and floor beams. STs were mounted to the top and bottom flanges of the through-girders at midspan and on the bottom flanges of the girders at the north quarter points. They were typically placed 3.2 cm

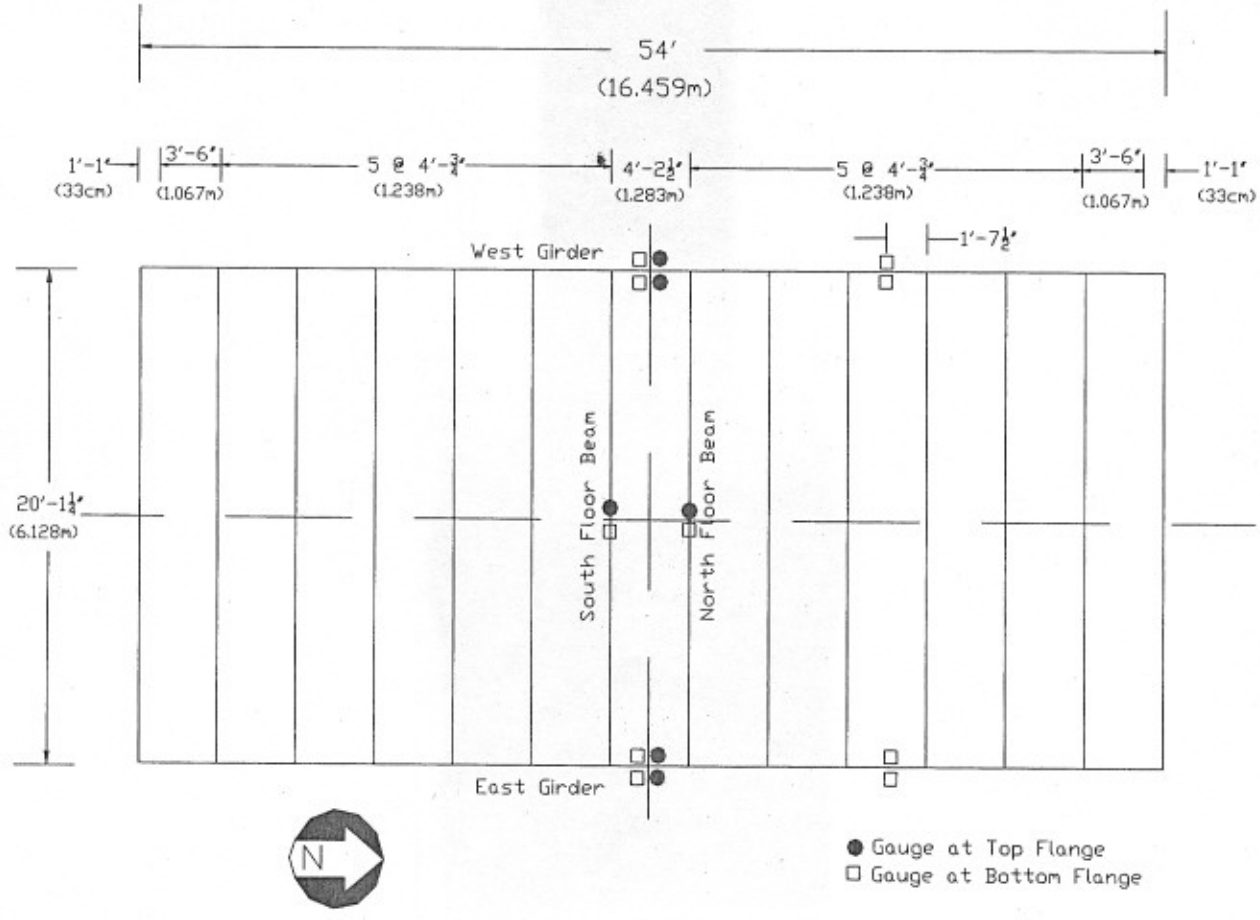

FIGURE 2 Plan view indicating strain transducer locations, Bridge #21.

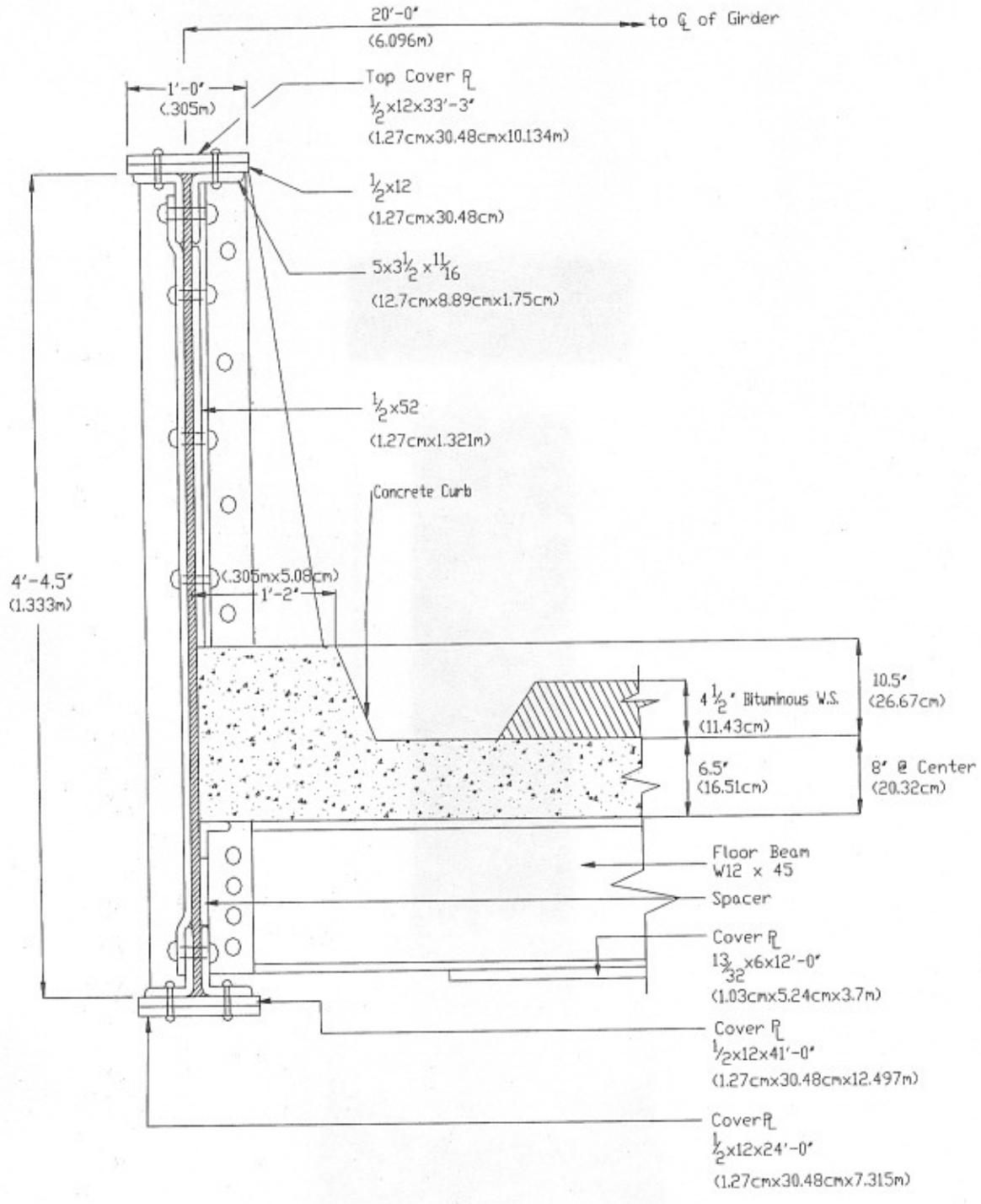

FIGURE 3 Half cross section, Bridge #21.

(1¼ in.) from the flange tips. At midspan, the transducers were placed on the outer faces of the top and bottom flanges for a total of four transducers per instrumented section. This placement scheme permitted examination of

- Level of strain at the extreme fibers of the cross section under load,
- Effect of the deck and curbing on flexural behavior, and
- Development of out-of-plane bending (warping).

At the quarter points, the STs were mounted to the exterior face of the bottom flange for a total of two transducers per instrumented section. This scheme permitted evaluating strains in the tensile flange under load and also allowed warping behavior to be examined.

STs were mounted to the interior top flange surface and the exterior bottom flange surface at midspan of the floor beams for a total of two transducers per instrumented section. This scheme permitted examining strains in the top and bottom flange under load and the influence of the concrete deck, which rested directly on the floor-

beam top flanges, on flexural behavior. Relative vertical displacements at midspan of each through-girder were recorded using linear variable differential transformers (LVDTs). Transducer designations and locations are summarized in Table 1.

The bridge was tested using an unloaded and loaded single-axle dump truck with an axle spacing of 4.4 m (14 ft 4 in.) and front and rear axle weights of 33.6 kN (7.6 kips) and 47.6 kN (10.7 kips) when empty and 34.9 kN (7.8 kips) and 81.4 kN (18.3 kips) when full, respectively. The test truck was driven across the structure at both crawl and posted (25-mph) speeds in the north-to-south and the south-to-north directions along three separate transverse paths for each test: (*a*) 2.4 to 2.2 m (8 ft 2 in. to 7 ft 4 in.) west of the centerline of the roadway; (*b*) 2.5 to 2.4 m (8 ft 4 in. to 7 ft 10 in.) east of the centerline of the roadway; and (*c*) straddling the roadway centerline. A total of 26 individual tests were performed—13 tests with the truck empty and 13 with the truck full.

DATA PROCESSING

The collected field data were processed in three steps:

1. Spectral analysis and data filtering,
2. Calculation of static flexural response, and
3. Determination of dynamic load allowance (DLA) values for each truck pass.

TABLE 1 Transducer Summary

Inst. #	Location	Inst. #	Location
ST-1	East Through-Girder at Mid-Span, West Top Flange Tip	ST-10	West Through-Girder at Mid-Span, East Bottom Flange Tip
ST-2	East Through-Girder at Mid-Span, East Top Flange Tip	ST-11	West Through-Girder at North Quarter Point, West Bottom Flange Tip
ST-3	East Through-Girder at Mid-Span, West Bottom Flange Tip	ST-12	West Through-Girder at North Quarter Point, East Bottom Flange Tip
ST-4	East Through-Girder at Mid-Span, East Bottom Flange Tip	ST-13	North Mid-Span Floor Beam at Mid-Span, South Bottom Flange Tip
ST-5	East Through-Girder at North Quarter Point, West Bottom Flange Tip	ST-14	North Mid-Span Floor Beam at Mid-Span, South Top Flange Tip
ST-6	East Through-Girder at North Quarter Point, East Bottom Flange Tip	ST-15	South Mid-Span Floor Beam at Mid-Span, South Bottom Flange Tip
ST-7	West Through-Girder at Mid-Span, West Top Flange Tip	ST-16	South Mid-Span Floor Beam at Mid-Span, South Top Flange Tip
ST-8	West Through-Girder at Mid-Span, East Top Flange Tip	LVDT-1	East Through-Girder at Mid-Span
ST-9	West Through-Girder at Mid-Span, West Bottom Flange Tip	LVDT-2	West Through-Girder at Mid-Span

The static response was isolated by removing the dynamic, higher-frequency components of the response using a Butterworth low-pass filter. The Butterworth filter offers the best approximation of the ideal response for low frequencies (*7*). The cutoff frequency was chosen based on evaluation of the spectral analysis results to ensure that the static response was retained. To determine the DLA for each truck pass, the maximum static strain obtained from the static strain time-history was compared with the maximum dynamic strain obtained from the dynamic time-history (*8, 9*).

NUMERICAL MODEL

A numerical, grillage-type model was developed using STAAD/Pro that models the through-girders and the floor beams as beam elements and the concrete deck as quadrilateral, finite plate and shell elements. All beam and plate elements are positioned in the same horizontal plane. Through-girder boundary conditions were modeled as simply supported with the south supports as pins restricting translation in three directions and the north supports as rollers. All steel was assumed to have an elastic modulus of 200 GPa (29,000 ksi), and geometric properties were calculated using field-measured dimensions and following relevant AASHTO guidelines for composite sections.

When faced with modeling an existing bridge, engineers generally use the original design plans to determine how the model should be constructed (i.e., noncomposite versus composite). However, if it can be demonstrated that a quantifiable level of composite behavior exists within certain structure types, then more informed decisions about the model could be made. Comparisons made herein are the first step in identifying if quantifiable levels of unintended composite action exist in through-girder bridges.

The model was evaluated with two separate analyses using both noncomposite and composite behavior. For the noncomposite analysis, through-girder and floor-beam section properties were set equal to those calculated for the steel sections alone. The composite analysis incorporated through-girder and floor-beam properties calculated to include a portion of the concrete deck. Integrating composite section properties in conjunction with plate elements effectively overstiffened the numerical model relative to the actual structure by 1% of the through-girder composite stiffness and 6% of the floor beam composite stiffness. This was considered acceptable.

Simulated truck bridge crossings in the numerical model corresponded with field test truck transverse positions. Analyses of field-tested members were performed, including member force and girder displacement calculations, at specified truck increments.

DISCUSSION OF RESULTS

Noncomposite and composite numerical model results are presented in conjunction with measured results when the test truck traveled in the south-north direction and was positioned along the centerline of the roadway (Test 24). Measured through-girder and floor-beam strains and girder midspan displacements are compared with predicted values from the numerical models in Figures 4 through 7.

Through-Girders

The degree of interaction between the concrete deck and curbing and the through-girders can be observed by comparing measured and

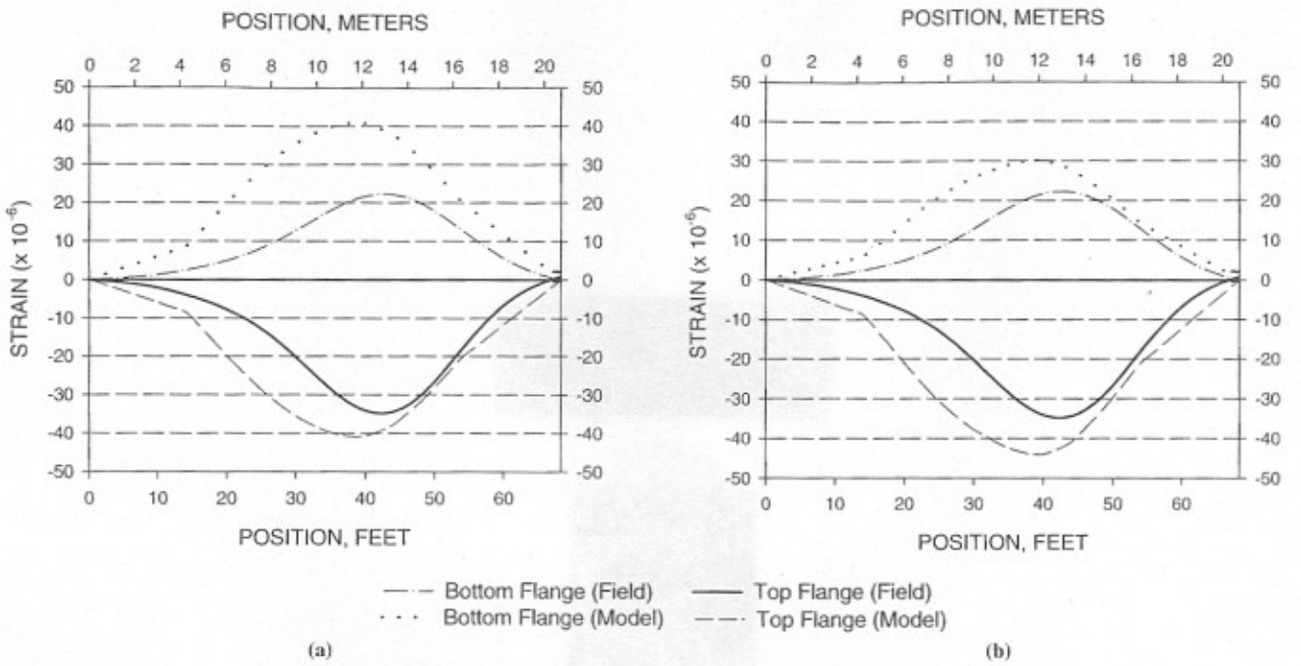

FIGURE 4 Through-girder strains versus front axle position, east through-girder: (*a*) noncomposite numerical model and (*b*) composite numerical model.

numerical results. Extreme fiber bending strain variation at midspan of the east through-girder versus truck position derived from the field test, the noncomposite numerical model, and the composite numerical model is shown in Figure 4. In addition, the vertical variation of strain and the location of the bending neutral axis are determined from Figure 6*a*. From these figures, it is observed that vertical strain distribution is not symmetrical for the symmetrical through-girder cross section. Compression (top) flange strain magnitudes are typically larger than strains observed for the tension (bottom) flange. Figure 6*a* indicates that the east through-girder neutral axis is not at midheight but below midheight and nearer the slab. When composite action is incorporated, the numerical model neutral axis location of 12.7 cm (5 in.) below midheight corresponds well with the measured neutral axis location of 15.2 cm (6 in.) below midheight. The

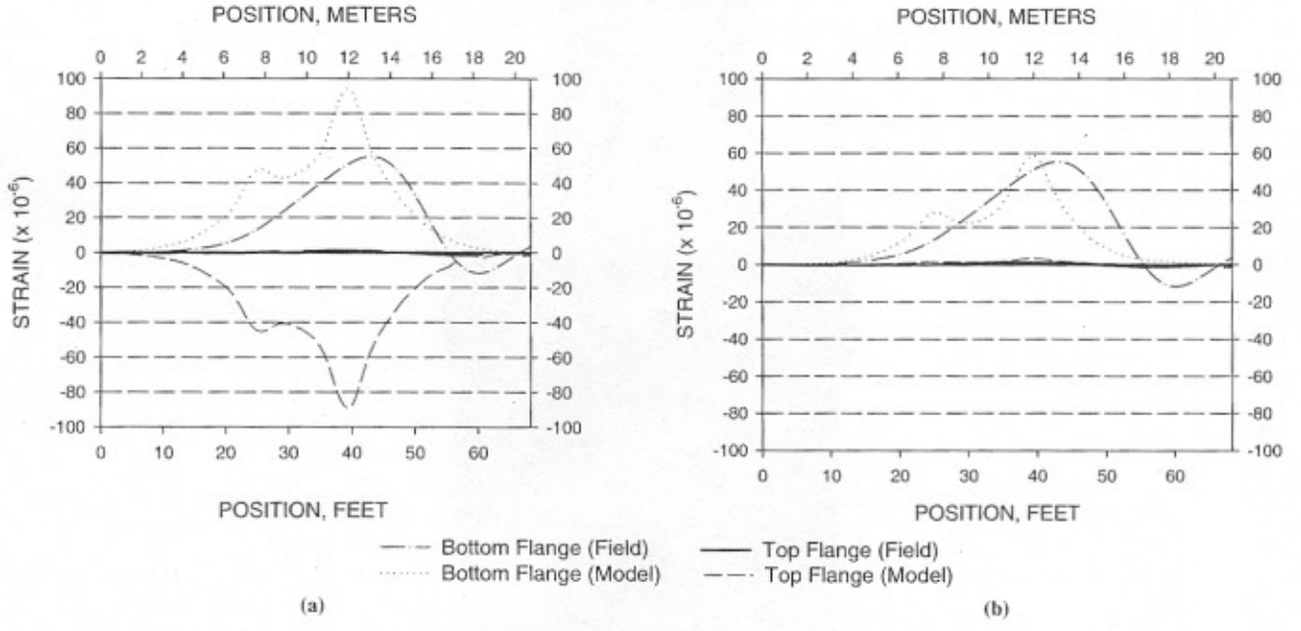

FIGURE 5 Floor-beam strains versus front axle position, south midspan floor beam: (*a*) noncomposite numerical model and (*b*) composite numerical model.

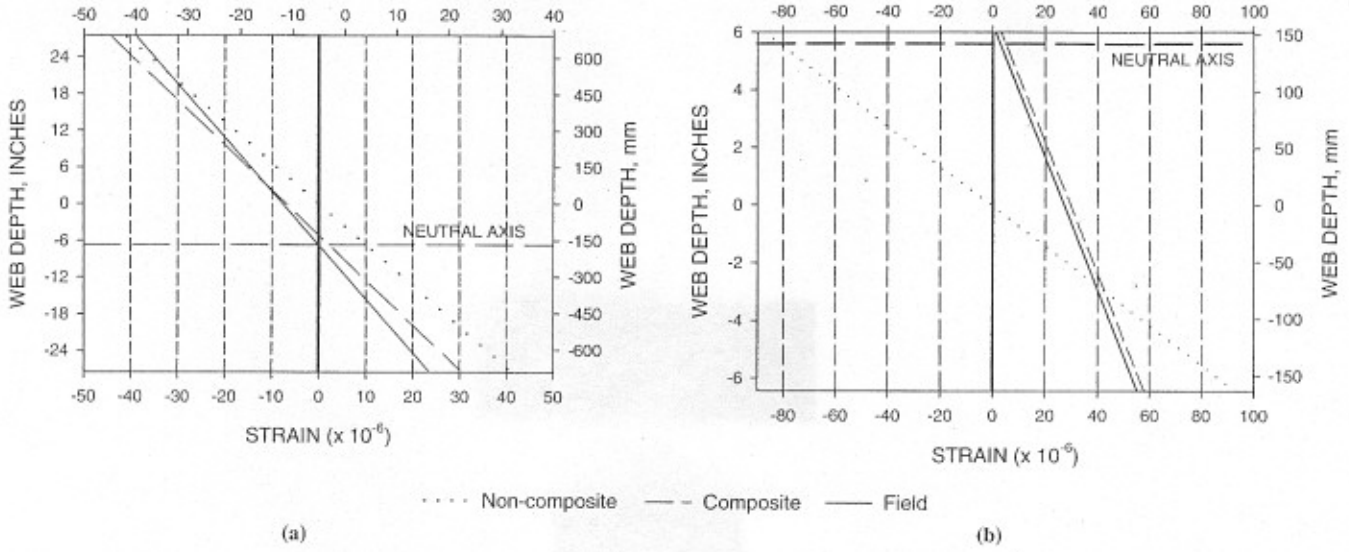

FIGURE 6 Midspan strain variations along (*a*) east through-girder section and (*b*) south midspan floor beam.

cause for the unsymmetrical strain distribution is shear transfer between the concrete deck and the through-girder web.

Floor Beams

Observations similar to those discussed previously for the through-girders can be made for the floor beam by inspection of Figure 5. The measured response in the figure indicates that the floor-beam neutral axis is nearly at the top flange with the entire cross section predominantly in tension, with small or nonexistent compression zones. As was discussed for the through-girders, the nonsymmetrical vertical strain variation indicates that the floor-beam neutral axis is not located at the position predicted for noncomposite behavior of the cross section. This is apparent because the composite model predicts the measured response more accurately than the noncomposite model. These results are substantiated using Figure 6*b*, which plots midspan noncomposite and composite strains through the depth of the south midspan floor beam. The slope of the noncomposite model strain-variation curve is much lower than the field data plot. However, the composite numerical model gives a slope parallel to the field data; the two plots are nearly identical. The floor-beam strain variations verify the field results: composite action does exist between the floor beams and concrete slab and the interaction is at a level that shifts the neutral axis near the top flange and slab interface. In fact, the composite model predicts the neutral axis location within the concrete slab at approximately 16.5 cm (6½ in.) above midheight, slightly larger than the 15.2-cm (6-in.) shift indicated by the field test.

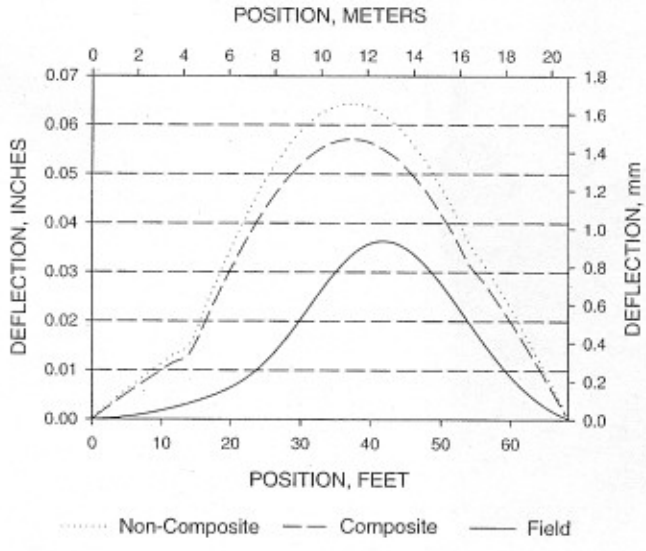

FIGURE 7 Midspan vertical deflection versus front axle position, east through-girder.

Through-Girder Displacements

Variations in through-girder midspan displacements are presented in Figure 7. Measured maximum displacements are smaller than corresponding composite and noncomposite numerical model predictions by 45% and 38%, respectively. Numerically derived displacements using composite properties resulted in a maximum displacement of approximately 1.7 mm (0.07 in.) and using noncomposite conditions 1.5 mm (0.06 in.). These deflections are significantly higher than the maximum measured 0.9-mm (0.036-in.) displacement (average of east- and west-girder deflections) and can be attributed to end-restraint developing at the bearing supports due to corrosion and deterioration of the structure over time and to the structure distributing loads more efficiently than the models could predict. Computer model boundary conditions and levels of discretization were not modified to account for these discrepancies.

Comparison of Numerical and Measured Strains

It is also observed that numerical model strain results are typically larger than measured strains by 5% to 70%, indicating an ability for the actual structure to distribute load more efficiently than the numerical models would predict. The numerical model incorporating noncomposite members poorly predicts the measured behavior, with a peak bottom flange tensile strain of approximately 95 με, whereas the measured peak value is 55 με, overestimating the strains by 73%.

The noncomposite numerical model also predicts a peak top flange strain near –90 με, which differs significantly from the field-measured value of 1.2 με, largely due to the location of the neutral axis. The composite model, which predicts a maximum floor-beam bottom flange strain of approximately 59 με and a peak top flange strain near 3 με, closely matches the measured values of 55 με and 1.2 με. It also can be observed that both the noncomposite and the composite numerical model results articulate the truck axles as they pass over the instrument locations. The measured strains did not articulate the axles because of the ability of the structure to distribute load to other members through the deck. Composite model results could be improved if more sophisticated computer models that include the deck were used. This work, however, focused only on the accuracy of simplified grillage models.

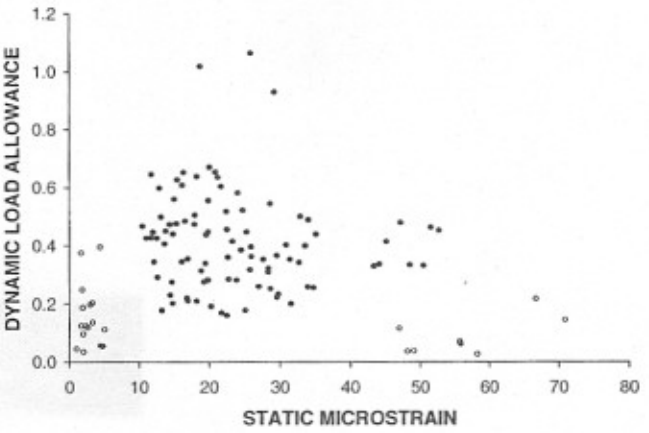

FIGURE 8 DLA versus peak static strain for test truck loading (through-girder DLA = •, floor-beam DLA = ○).

Dynamic Load Allowance

Past studies (*8–10*) have shown a relationship between peak static stress and bending DLA. To consider the relationship between DLA values and peak static strain for the present study, bending DLA is plotted as a function of peak static strain for both the through-girders and the floor beams in Figure 8. The graph presents response data derived from four passes of the empty test truck and four passes of the loaded test truck. The measured DLA represents the current level of dynamic response to the test vehicle rather than an anticipated 75-year design-level response. Due to the extremely low truck volume, data under normal traffic could not be collected.

The measured bending through-girder DLA values exhibit a relatively wide scatter over the range of peak static stress. A weak negative correlation between decreasing DLA and increasing peak static strain is observed, with a DLA average of 0.4. This behavior is consistent with previous studies conducted on straight, steel I-girder bridges (*8*), through-truss bridge floor systems (*9*), and prestressed concrete I-girder bridges (*10*) and is also described in *NCHRP Synthesis of Highway Practice 266* (*11*). The measured bending DLA values for the floor beam exhibit a clear trend between the strains measured near the neutral axis (less than 10 με) and the strains measured at the bottom flange (greater than 40 με). The present study exhibits a somewhat weaker correlation than the cited studies. However, data presented in Figure 8 are over a narrower range of static strain due to a single truck and indicate a decreasing DLA with increasing peak static strain, providing evidence to support the AASHTO impact factor (IM) of 33%.

LOAD RATING

To investigate the effects of composite action on the capacity of the girders and floor beams, load ratings were performed using recorded live-load strains. Load rating calculations were conducted following procedures outlined in the AASHTO *Manual for the Maintenance Inspection of Bridges* (*12*). Strains were converted to live-load stresses and scaled to an AASHTO H15 truck following a method outlined by Boothby and Craig (*13*). Maximum girder and floor-beam strains from the crawl tests were used. Dead-load stresses were estimated using dimensions and unit weights from a load rating of the bridge completed by Greiner Engineering Sciences, Inc. (*14*). Calculations were initially performed assuming no section loss in the members, which matches assumptions made by Greiner. Results from the current calculations are compared with those completed by Greiner in the first two rows of Table 2. These results clearly show the effects of composite action on the capacity of the girders and floor beams. Interaction between the deck and girder web has increased the girder capacity approximately 25% over that predicted from the 1984 load ratings. Composite action for the floor beams has a more dramatic effect, increasing the beams' capacity more than four times that predicted in 1984.

To evaluate if beneficial effects of unintended composite action in the floor beams could be overcome, horizontal shear stresses at top flange and deck interface were estimated following criteria outlined in the *Manual for Bridge Rating Through Load Testing* (*15*). These calculations conservatively gave a shearing stress of 503 kPa (73 psi) for the test truck, which is only slightly above the 482 kPa (70 psi) limit given in the manual for top flanges not embedded in the deck.

Levels of section loss observed in the floor beams during the field test would alter the values shown for Rating 2 in Table 2. To investigate the effect of section loss on the floor-beam ratings, they were recalculated using reduced section properties from a rating performed by the Chester County Engineers Office (*16*). The Chester County ratings reduced full section properties calculated by Greiner using field measurements. Based on the field measurements, it was assumed that the floor beams had 15% section loss. Reducing geometric properties accordingly and recalculating the field test ratings

TABLE 2 Load Rating Comparisons, H15 Truck, of Field Test with Greiner Ratings (*14*)

		Field Test		Greiner[b]	
Rating	Member	Inventory (Mg[a])	Operating (Mg)	Inventory (Mg)	Operating (Mg)
1	Girder	54.9	91.6	43.3	72.5
2	Floor Beam	28.7	51.7	6.3	11.4
3	Floor Beam – 15% Loss	27.2	49.9	5.4[#]	9.7[#]

[a] 1 Mg = 1.1 ton.
[b] Greiner ratings recalculated using 15% section loss by Chester Co.

gave the values shown for Rating 3 in Table 2, which are compared with 1996 Chester County ratings. The results indicate that the level of section loss that was apparent in the floor beams did reduce the ratings but not to the point at which they became critical. For floor-beam operating ratings to be below the gross vehicle weight of an H15 truck, approximately 80% section loss would have to occur if maximum live-load stresses from the field tests, which account for composite action, were used in the calculations. These results are dramatically different from those obtained by Chester County, which do not account for any composite action.

CONCLUSIONS

The composite section numerical model strain and deflection predictions were relatively accurate as compared with the field data, indicating that interaction is occurring between the concrete deck and the steel superstructure. This observation is significant because the bridge was not initially designed to behave compositely and may allow a higher posting level because of the unintended composite action caused by friction and chemical bond between the deck and steel superstructure. Although not examined explicitly, the frictional component would increase proportionally with live load except at extreme overload, when the frictional resistance to slip could be overcome. The level at which this occurs is structure-specific, and engineers should attempt to examine bridge usage, location, and historical records about overload conditions before making any final decisions about posting level changes.

The composite section numerical model accurately predicted neutral axes locations for both the girders and floor beams. Neutral axes were shown to shift from midheight, indicative of composite behavior.

Both composite and noncomposite section numerical models predicted similar girder displacement values. However, the models significantly overestimated peak midspan displacements due to idealization of support conditions and the ability of the actual structure to distribute load more efficiently than the simplified models would predict. Engineers should be aware of the effects of end conditions and continuity when using simplified models to estimate bridge response.

Based on the relative accuracy with which bridge-member strains and deflections were predicted, the relatively low level of analysis demonstrated competency in its ability to accurately analyze Chester County Bridge #21. As a cost-efficient technique to analyze a structure for strength and behavior, numerical models of the type used in the present study can predict stresses with relative accuracy.

The measured DLA for the bridge members contained significant scatter; however, as the peak static strain increased, a decreasing trend in the DLA was observed. This observation is consistent with other published studies.

The benefit of the level of composite action present in Bridge #21 was demonstrated through calculation of revised load ratings for the girders and floor beams. These ratings accounted for composite action by incorporating field-measured live-load stresses into the calculations. They indicated that the existing posting of the bridge is conservative at the load levels at which it was tested and rated. Although care should be exercised if the bridge is subjected to an overload event, these results do indicate that unintended composite action should be examined as a viable alternative to posting through-girder bridges that initially appear functionally obsolete.

ACKNOWLEDGMENTS

The authors acknowledge the support and assistance provided by Ben Craddock of the Chester County Engineers Office. The assistance of Charles Leighty and Arthur Fritch with completion of the field testing and of Elizabeth Norton with reducing the field data is also greatly acknowledged.

REFERENCES

1. Aktan, A. E., D. N. Farhey, and V. Dalal. Issues in Rating Steel-Stringer Bridges. In *Transportation Research Record 1476*, TRB, National Research Council, Washington, D.C., 1995, pp. 129–138.
2. Bakht, B., and L. G. Jaeger. Bridge Testing: A Surprise Every Time. *Journal of Structural Engineering*, Vol. 115, No. 5, May 1990, pp. 1370–1383.
3. Chajes, M. J., D. R. Mertz, and B. Commander. Experimental Load Rating of a Posted Bridge. *Journal of Bridge Engineering*, Vol. 2, No. 1, Feb. 1997, pp. 1–10.
4. Zhou, Y. E. Load Testing and Strength Evaluation of a Non-Composite Steel Plate Girder Bridge. *Proc., ASCE Structures Congress*, Chicago, Ill., April 1996, pp. 884–891.
5. Linzell, D. *Field Testing of Bridge #21—Muddy Run Road over Muddy Run*. Report PTI 2001-17. Pennsylvania Transportation Institute, University Park, Aug. 2000.
6. *Recording and Coding Guide for the Structure Inventory and Appraisal of the Nation's Bridges*. Report FHWA-PD-96-001. Office of Engineering, Bridge Division, FHWA, U.S. Department of Transportation, 1995.
7. Johnson, D. E., J. R. Johnson, and H. P. Moore. *A Handbook of Active Filters*. Prentice Hall, Englewood Cliffs, N.J., 1980.
8. Kim, S., and A. Nowak. Load Distribution and Impact Factors for I-Girder Bridges. *Journal of Bridge Engineering*, Vol. 2, No. 3, Aug. 1997, pp. 97–104.
9. Laman, J. A., J. S. Pechar, and T. E. Boothby. Dynamic Impact Factors for Through-Truss Bridges. *Journal of Bridge Engineering*, Vol. 4, No. 4, Nov. 1999, pp. 231–241.
10. Schwarz, M. J., and J. A. Laman. Response of Prestressed Concrete I-Girder Bridges to Live Load. *Journal of Bridge Engineering*, Vol. 6, No. 1, Jan./Feb. 2001, pp. 1–8.
11. McLean, D. I., and M. L. Marsh. *NCHRP Synthesis of Highway Practice 266: Dynamic Impact Factors for Bridges*. TRB, National Research Council, Washington, D.C., 1998.
12. *Manual for the Maintenance Inspection of Bridges*. AASHTO, Washington, D.C., 1993.
13. Boothby, T. E., and R. J. Craig. Experimental Load Rating Study of a Historic Truss Bridge. *Journal of Bridge Engineering*, Vol. 2, No. 1, Feb. 1997, pp. 18–26.
14. *Chester County Bridge #21 Rating*. Greiner Engineering Sciences, Inc., King of Prussia, Pa., 1984.
15. *NCHRP Research Results Digest 234: Manual for Bridge Rating Through Load Testing*. TRB, National Research Council, Washington, D.C., Nov. 1998.
16. *Bridge #21 Floor Beam Analysis*. Chester County Engineers Office, West Chester, Pa., 1996.

Publication of this paper sponsored by Committee on Dynamics and Field Testing of Bridges.